

A Simple Long-Tailed Recognition Baseline via Vision-Language Model

Teli Ma¹, Shijie Geng¹, Mengmeng Wang¹, Jing Shao², Jiasen Lu³
Hongsheng Li⁴, Peng Gao^{†1}, Yu Qiao¹

¹Shanghai Artificial Intelligence Laboratory ²SenseTime Research

³PRIOR@Allen Institute for AI ⁴The Chinese University of Hong Kong

{mateli, gaopeng, qiaoyu}@pjlab.org.cn

Abstract

The visual world naturally exhibits a long-tailed distribution of open classes, which poses great challenges to modern visual systems. Existing approaches either perform class re-balancing strategies or directly improve network modules to address the problem. However, they still train models with a finite set of predefined labels, limiting their supervision information and restricting their transferability to novel instances. Recent advances in large-scale contrastive visual-language pretraining shed light on a new pathway for visual recognition. With open-vocabulary supervisions, pretrained contrastive vision-language models learn powerful multimodal representations that are promising to handle data deficiency and unseen concepts. By calculating the semantic similarity between visual and text inputs, visual recognition is converted to a vision-language matching problem. Inspired by this, we propose **BALLAD** to leverage contrastive vision-language models for long-tailed recognition. We first continue pretraining the vision-language backbone through contrastive learning on a specific long-tailed target dataset. Afterward, we freeze the backbone and further employ an additional adapter layer to enhance the representations of tail classes on balanced training samples built with re-sampling strategies. Extensive experiments have been conducted on three popular long-tailed recognition benchmarks. As a result, our simple and effective approach sets the new state-of-the-art performances and outperforms competitive baselines with a large margin. Code is released at <https://github.com/gaopengcuhk/BALLAD>.

1. Introduction

During past years, visual recognition tasks, such as image classification [21, 58, 65], object detection [36, 53], semantic segmentation [5, 42, 74], and instance segmentation [20, 24, 40] have been significantly improved. The performance

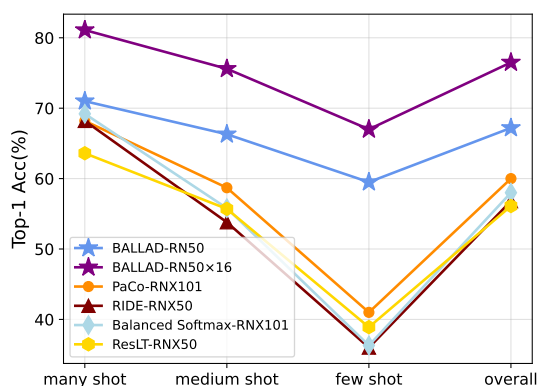


Figure 1. Comparison with the state-of-the-art approaches on ImageNet-LT. BALLAD with ResNet-50 visual backbone outperforms state-of-the-art models which have more complex backbones and longer training epochs by a large margin (up to +7.2% improvement on overall accuracy compared with PaCo [10]), especially for categories without abundant training examples. BALLAD with ResNet-50×16 achieves a new state-of-the-art performance of 76.5% top-1 accuracy on ImageNet-LT benchmark dataset. (RN50: ResNet-50, RN50×16: the EfficientNet method with 16× compute of ResNet-50, RNX50: ResNeXt-50, RNX101: ResNeXt-101.)

gains can be largely attributed to the availability of large-scale high-quality datasets [12, 33, 38]. However, the problem of data imbalance has inevitably emerged since real-world data often abide by a long-tailed distribution (e.g., Pareto distribution [49] or Zipf’s law [78]). In other words, a few head classes dominate the majority of training examples, whereas many rare or fine-grained classes only have limited relevant data points.

To alleviate the issue, previous efforts either carefully create more balanced datasets (e.g., ImageNet [12], MSCOCO [38], and Kinetics-400 [31]) with human labors or develop more robust algorithms to handle data imbalance. However, since the former is notoriously laborious and expensive, many researchers have been devoted to the latter. Formally, long-tailed recognition (LTR) is a research

field seeking robust models that 1) are resistant to significant imbalanced class distribution; 2) can deal with few-shot learning of tail classes. Many methods [73] have been proposed for solving LTR problems. According to the core technical contributions, they can be divided into two categories. Methods in the first line focus on class re-balancing strategies [22, 29, 44, 70] such as data re-sampling, loss re-weighting, and logit adjustment. The second category focuses on improving network modules [9, 10, 30, 54, 59, 72, 75] by classifier designing, decoupled training, and representation learning. While these methods have achieved significant progress, the performance of LTR remains unsatisfactory. When delving deeper into the utilization of the existing imbalance datasets, we have observed that almost all previous efforts are confined to a predetermined manner which designs models entirely relying on the visual modality. That is to say, they totally ignore the semantic features of the raw label text, which may be a promising solution to exert additional supervision on inadequate data sources. Therefore, this paper explores whether language modality can be effective and complementary information for this task. In the meantime, we could broaden generalization abilities to few-shot categories and zero-shot novel instances.

Recently, contrastive vision-language models such as CLIP [51] and ALIGN [26] brought a breath of fresh air into the vision community. They learn to align vision and language representations with a contrastive loss given large-scale noisy image-text pairs collected from the web. The powerful visual-language representations obtained from pre-training significantly improve the zero-shot classification performance in open-vocabulary settings without any additional annotations. Motivated by the success of contrastive vision-language models and the curiosity of the language effect mentioned above, we directly test CLIP on LTR datasets under its zero-shot setting. Surprisingly, the results are balanced on many-shots (59.4%), medium-shots (57.5%), and low-shots (57.6%) subsets of ImageNet-LT [41] and the overall performance (58.2%) is comparable to the state-of-the-art [10]. From which we see the great potential of the multimodality solution for LTR. To further improve the performance while keep the capability of dealing with data imbalance, an intuitive way is to finetune the vision-language models on LTR datasets. However, we find it only brings a slight gain. Therefore, the core task of our work becomes *how to design an effective recipe for training vision-language models under the circumstances of long-tailed distribution*.

Specifically, in this paper, we design a simple framework based on contrastive vision-language models for LTR. The training procedure of the framework is broken into two phases from the perspective of distribution skewness: A) utilizing abundant annotations from LTR datasets; B) tackling few-shot learning of tail classes on balanced data built with re-sampling strategies. In Phase A, we continue pre-

training CLIP backbone on a specific LTR dataset through contrastive learning. It enables our framework to fully exploit available training examples and update visual-language representations on a new domain. To further facilitate the few-shot learning of tail classes, during Phase B, we freeze the CLIP backbone and employ an auxiliary linear adapter for finetuning on re-balanced training samples. The adapter dynamically combines fixed Phase-A and finetuned Phase-B features via a residual connection to refine the visual representations of tail classes. Compared with finetuning the whole CLIP backbone directly, the linear adapter reduces the number of learnable parameters and thus prevents the potential overfitting of few-shot setups. According to Figure 1, our framework clearly achieves better performances than state-of-the-art LTR approaches. The improvements are especially significant for few-shot and medium-shot classes, demonstrating our approach’s great capability of handling class imbalance. Since our framework solves the data imbalance via a linear adapter, we name it as **BALLAD (BALanced Linear ADapter)**, which implies the harmony of head and tail classes. Our contributions are three folds:

- We point out the shortcomings of training with fixed class labels and propose to leverage language modality via contrastive vision-language backbone to facilitate long-tailed recognition.
- We develop the BALLAD framework consisting of two phases to handle head and tail classes successively. Specifically, we keep training the visual and language branches of the pretrained vision-language model simultaneously at the first stage. Then we adopt a linear adapter to tackle tail classes with vision-language parameters frozen.
- We conduct extensive experiments to demonstrate the effectiveness of BALLAD. Our simple baseline achieves the new state-of-the-art performances on all benchmarks, outperforming the old paradigm by 16.5 points maximally on ImageNet-LT.

2. Related Work

Contrastive Vision-Language Model. Contrastive representation learning has been widely adopted to fulfill self-supervised pretraining in various AI domains [3, 4, 6, 17, 19, 47]. Recently, the intersection of vision and language [1, 7, 16, 32, 46, 55, 68] also experienced a revolution sparked by contrastive representation learning. Contrastive vision-language models like CLIP [51] and ALIGN [26] demonstrate promising zero-shot performances on various visual search and recognition tasks. Learning directly from natural language supervisions that contain rich visual concepts, they are very flexible and robust to distribution variations across different domains. The success of CLIP and ALIGN has enlightened many downstream vision-language tasks. For instance, DeCLIP [35] proposes to utilize self-

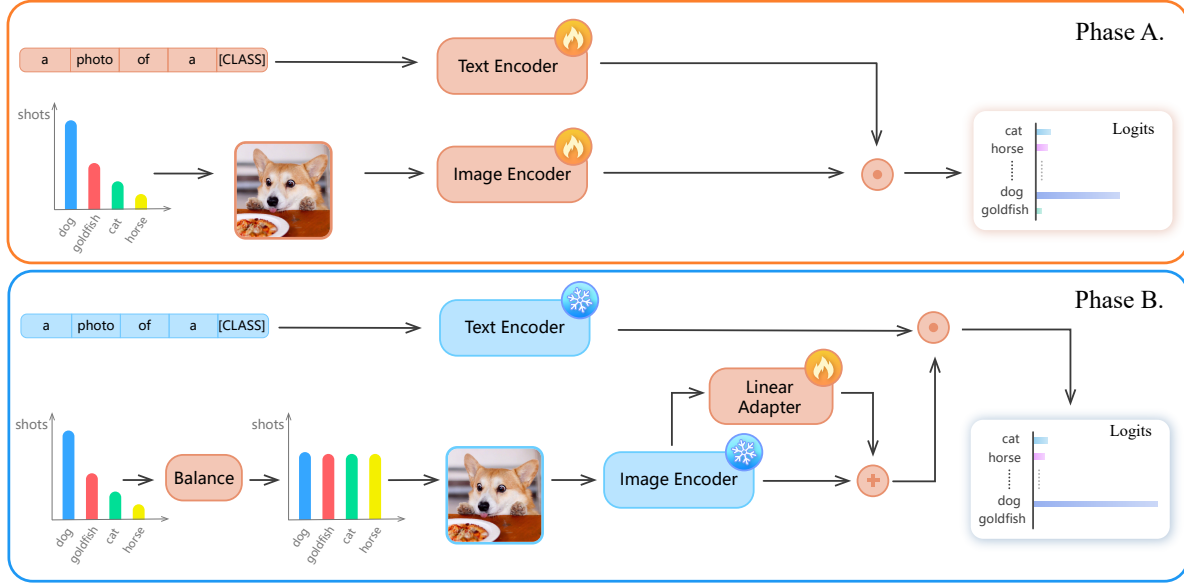


Figure 2. Overview of our BALLAD framework. In Phase A, we keep pretraining the text and image branches of the vision-language backbone on long-tailed data. After Phase A, head classes typically achieve good enough classification performance, whereas tail classes are still far from perfect. During Phase B, a linear adapter is adopted to further train the vision-language backbone on balanced training samples. As a result, tail classes enjoy a performance boost while head classes slightly increase or maintain their original classification accuracy. 🔥 represents training with parameter update while ❄️ represents freezing parameters.

multi-view, and nearest-neighbor supervisions among the image-text pairs for data efficient pretraining of CLIP. On visual classification tasks, CLIP-Adapter [15] argues that fine-tuning contrastive vision-language models with linear adapters is a better alternative to prompt tuning. For video related tasks, VideoCLIP [66] performs contrastive pretraining with video-text pairs for zero-shot video-text understanding. ActionCLIP [61] presents a new “pretrain, prompt and fine-tune” paradigm leveraging pretrained vision-language models for zero-shot/few-shot action recognition. CLIP-It [45] designs a language-guided multimodal transformer based on CLIP to address query-focused video summarization. Moreover, CLIPort [57] combines CLIP with Transporter [69] to endow a robot with the ability of semantic understanding and spatial perception. In this paper, we demonstrate that contrastive vision-language models can also facilitate visual recognition under long-tailed class distribution setups if properly trained.

Long-Tailed Recognition. Long-tailed recognition [73] is a practical and challenging problem in vision domain. General visual models will suffer from severe performance degradation under such imbalanced class distributions. A great number of approaches [9, 10, 13, 25, 44, 48, 54, 63, 67, 71] have been proposed to address LTR from different perspectives. An intuitive solution is to directly re-balance the number of training samples across all classes [30, 75]. However, naively adjusting the skewness of training samples may lead to the overfitting of tail classes. Better alternatives include loss re-weighting [22, 29, 37] and logit adjustment [44, 70] based

on label frequencies. Though efficacious for long-tailed distribution, above methods all sacrifice the performance of head classes at varying levels. To address the limitations, researchers turn to explore new network architectures and training paradigms. Typically, long-tail recognition models contain two key components – feature extractor and classifier. For each component, there are corresponding approaches by either designing better classifier [39, 59, 64] or learning reliable representations [41, 77]. In terms of new training frameworks, existing efforts seek to divide a one-stage training paradigm into two stages. For example, decoupled training approaches [28, 30] conduct representation learning and classifier training in a separate manner. Furthermore, ensemble learning schemes [72, 75] first learn multiple experts with different data sub-groups and then merge their complementary knowledge to handle LTR. In contrast, our BALLAD first utilizes abundant long-tailed data to refine visual-language representations on a new target domain. Then we apply a lightweight linear adapter to encourage fine-grained representation learning from balanced samples. The two phases successively handle the learning of head and tail classes and ensure a better balanced performance across all classes.

3. Our Method

In this section, we first briefly revisit how contrastive vision-language models leverage contrastive objectives to achieve efficient and scalable multimodal representation learning. Moreover, we formally present BALLAD frame-

work and discuss the advantages of the proposed two-stage representation learning for long-tailed class distributions.

3.1. Contrastive Vision-Language Model

Contrastive vision-language models such as CLIP [51] and ALIGN [26] typically follow a dual-encoder architecture with a language encoder \mathcal{L}_{enc} and a visual encoder \mathcal{V}_{enc} . Given an input image \mathbf{I} , \mathcal{V}_{enc} is adopted to extract the visual feature for \mathbf{I} : $\mathbf{f}_v = \mathcal{V}_{\text{enc}}(\mathbf{I}) \in \mathbb{R}^{d_v}$. Likewise, \mathcal{L}_{enc} is applied to encode an input text sequence \mathbf{T} into its corresponding text feature: $\mathbf{f}_l = \mathcal{L}_{\text{enc}}(\mathbf{T}) \in \mathbb{R}^{d_l}$. After extracting the feature for each modality, two transformation matrices $\mathbf{W}_v \in \mathbb{R}^{d_v \times d}$ and $\mathbf{W}_l \in \mathbb{R}^{d_l \times d}$ are employed to project the original visual and text features into a shared embedding space:

$$\mathbf{v} = \frac{\mathbf{W}_v^\top \mathbf{f}_v}{\|\mathbf{W}_v^\top \mathbf{f}_v\|}, \quad \mathbf{u} = \frac{\mathbf{W}_l^\top \mathbf{f}_l}{\|\mathbf{W}_l^\top \mathbf{f}_l\|}, \quad (1)$$

where \mathbf{v} and \mathbf{u} are both d -dimension normalized vectors in the joint multimodal space. During pretraining, contrastive vision-language models learn to align image-text pairs inside a batch. The overall training objective consists of matching losses from two different directions, *i.e.*, $\mathcal{L}_{v \rightarrow l}$ for text retrieval and $\mathcal{L}_{l \rightarrow v}$ for image retrieval. They both maximize the scores of matched pairs while minimize that of unmatched ones:

$$\mathcal{L}_{v \rightarrow l} = -\frac{1}{N} \sum_i \log \frac{\exp(\mathbf{v}_i^\top \mathbf{u}_i / \tau)}{\sum_{j=1}^N \exp(\mathbf{v}_i^\top \mathbf{u}_j / \tau)}, \quad (2)$$

$$\mathcal{L}_{l \rightarrow v} = -\frac{1}{N} \sum_i \log \frac{\exp(\mathbf{u}_i^\top \mathbf{v}_i / \tau)}{\sum_{j=1}^N \exp(\mathbf{u}_i^\top \mathbf{v}_j / \tau)}, \quad (3)$$

where τ denotes the temperature hyperparameter and N represents the number of image-text pairs in the batch.

Trained with large-scale image-text pairs under the open-vocabulary settings, contrastive vision-language models achieve powerful multimodal representations and naturally possess the capability of zero-shot visual recognition. A collection of text descriptions following templates like "a photo of a {CLASS}" is created for candidate classes in target datasets to perform zero-shot prediction. If we represent the normalized test image feature as \mathbf{v} and all normalized text description features as $\{\mathbf{u}_1, \dots, \mathbf{u}_K\}$, we can thus compute the class probability of the test image as below:

$$p_i = \frac{\exp(\mathbf{v}^\top \mathbf{u}_i) / \tau}{\sum_{j=1}^K \exp(\mathbf{v}^\top \mathbf{u}_j) / \tau}, \quad (4)$$

where p_i represents the probability for class i , and K stands for the total number of candidate classes. Finally, the text label with the highest probability is selected as the prediction.

3.2. Balanced Linear Adapter

As stated in Section 1, contrastive vision-language models obtain balanced performance for head and tail classes, whereas traditional approaches like PaCo [10] suffer from lower performance of tail classes owing to the deficiency of training samples. Inspired by the zero-shot ability of contrastive vision-language models, we choose CLIP as our backbone for long-tailed recognition. The observation in Section 4.3.2 also encourages us to decouple the training of long-tailed data into two phases. To be specific, the first phase (Phase A) fully utilizes available training data and ensures the performance for classes with abundant examples, then the second phase (Phase B) focuses on improving the few-shot learning of tail classes. Note that LWS [30] also adopts a decoupled training framework. However, LWS decouples the training of representation and classifier into two stages. In contrast, our two phases are for long-tailed and balanced training samples respectively and both phases conduct representation refinement with contrastive loss.

Phase A. Recently, Gururangan *et al.* [18] shows that keeping domain-adaptive and task-adaptive model pretraining can largely improve the performances on target NLP tasks. Similarly, for our Phase A, we find that continuing the pretraining of contrastive vision-language backbone on long-tailed target dataset also benefits the learning of classes with abundant examples. In this way, Phase A can make full use of available training data regardless of its skewness. Since we focus on classifying input images into text labels, the pretraining of Phase A directly follows the loss defined in Equation (2). As shown in Figure 2, Phase A updates the representations of both text and image encoders on a new domain. After Phase A, head classes typically achieve good performance while tail classes still require another stage of balanced training.

Phase B. Tail classes are short of training examples and under the few-shot settings. Directly training the whole vision-language backbone may easily overfit to them and lead to performance degradation. Inspired by parameter-efficient adapter modules [23], we freeze the vision-language backbone obtained from Phase A and utilize an additional linear adapter layer to help our model refine its visual-language representation on those infrequent classes. As shown in Figure 2, the text features would remain the same as Phase A. The only difference lies in the image features. If we assume the original image feature to be \mathbf{f} , the weight matrix and bias of the linear adapter as $\mathbf{W} \in \mathbb{R}^{d \times d}$ and $\mathbf{b} \in \mathbb{R}^d$, then we can represent the refined image feature \mathbf{f}^* as

$$\mathbf{f}^* = \lambda \cdot \text{ReLU}(\mathbf{W}^\top \mathbf{f} + \mathbf{b}) + (1 - \lambda) \cdot \mathbf{f}, \quad (5)$$

where λ indicates the residual factor to dynamically combine Phase-B fine-tuned image features with the original image features of Phase A.

To avoid the Phase-B training from biasing towards head classes, we also adopt class-balanced sampling strategy [30]

to construct a balanced group of training samples. Suppose there are K classes that constitute a total of N training samples in the target dataset. We can represent the number of training samples for class j as n_j and thus have $N = \sum_{j=1}^K n_j$. If we assume these classes are already sorted in a decreasing order, then a long-tailed distribution implies $n_i \geq n_j$ if $i < j$ and $n_1 \gg n_K$. For class-balanced sampling, we define the probability of sampling each data point from class j to be $q_j = \frac{1}{K}$. In other words, to construct a balanced group of training samples, we will first uniformly choose a class out of the K candidates and then sample one data point from the selected class. Finally, we perform Phase B finetuning with $\mathcal{L}_{v \rightarrow l}$ on the balanced training data.

4. Experiments

4.1. Experiment Setup

Datasets. We conduct our experiments on three long-tailed benchmark datasets, namely ImageNet-LT [41], Places-LT [41], and CIFAR100-LT [2]. ImageNet-LT and Places-LT were first introduced in [41] for long-tailed recognition research. ImageNet-LT is a long-tailed dataset with 1,000 categories sampled from the original ImageNet [12] following the Pareto distribution with a power value of $\alpha = 6$. There are 115.8K images in the training split, with maximally 1,280 images per class and minimally 5 images per class. The testing split maintains the same as the original ImageNet [12], where samples per class are balanced. Places-LT is a long-tailed version of the original Places2 Database [76]. The training split of Places-LT contains with 184.5K images from 365 categories, with 4,980 images maximally per class and minimally 5 images per class. For the testing split, the images of each class is also balanced with 100 images per class. CIFAR100-LT [2] are created by long-tailed imbalance technique [11] which reduces training examples per class based on an exponential decay function. In this paper, we directly use the version from [63] with an imbalance ratio ρ of 100. The training split contains 50K images from 100 categories, while the testing split has a uniform 100 images for each class.

Implementation Details. We use CLIP as the contrastive vision-language backbone in all experiments. For the visual branch of CLIP, we vary among ResNet-50, ResNet-100, ViT-B/16, and ResNet-50 \times 16, which is 16 \times computation cost of ResNet-50 following the style of EfficientNet as introduced in [51]. The ResNet-50 is leveraged for all ablation studies by default unless specified. We use SGD as the optimizer for all experiments with a momentum of 0.9. The batch size is set to 512. We adopt cosine learning rate schedule to decay learning rates. The initial learning rate of CLIP finetuning is set to 1×10^{-5} for both the visual and language encoders, while the learning rate of linear adapter is set to 0.2 at the start. For data pre-processing, images are resized

Method	Backbone	#Epochs	Many	Medium	Few	All
τ -normalized [30]	ResNet-50	90	56.6	44.2	27.4	46.7
	ResNet-101	90	59.4	47.0	30.6	49.6
	ResNet-152	90	59.6	47.5	32.2	50.1
	ResNeXt-50	90	59.1	46.9	30.7	49.4
	ResNeXt-101	90	59.1	47.0	31.7	49.6
	ResNeXt-152	90	62.2	50.1	35.8	52.8
LWS [30]	ResNet-50	90	57.1	45.2	29.3	47.7
	ResNet-101	90	60.1	47.6	31.2	50.2
	ResNet-152	90	60.6	47.8	31.4	50.5
	ResNeXt-50	90	60.2	47.2	30.3	49.9
	ResNeXt-101	90	60.5	47.2	31.2	50.1
	ResNeXt-152	90	63.5	50.4	34.2	53.3
ResLT [9]	ResNeXt-50	180	63.0	50.5	35.5	52.9
	ResNeXt-101	180	63.3	53.3	40.3	55.1
Balanced Softmax [52]	ResNet-50	400	66.7	52.9	33.0	55.0
	ResNeXt-50	400	67.7	53.8	34.2	56.2
	ResNeXt-101	400	69.2	55.8	36.3	58.0
RIDE† [62]	ResNet-50	100	66.2	52.3	36.5	55.4
	ResNeXt-50	100	68.2	53.8	36.0	56.8
PaCo‡ [10]	ResNet-50	400	65.0	55.7	38.2	57.0
	ResNeXt-50	400	67.5	56.9	36.7	58.2
	ResNeXt-101	400	68.2	58.7	41.0	60.0
BALLAD	ResNet-50	50+10	71.0	66.3	59.5	67.2 (+7.2)
	ResNet-101	50+10	74.7	69.1	63.3	70.5 (+10.5)
	ViT-B/16	50+10	79.1	74.5	69.8	75.7 (+15.7)
	ResNet-50 \times 16	50+10	81.1	75.6	67.0	76.5 (+16.5)

Table 1. Long-tailed recognition accuracy on ImageNet-LT for different methods and backbones. The red colored numbers represent the improvement of overall accuracy compared with the state-of-the-art performance (PaCo with 60.0% overall accuracy). †: RIDE uses 4 experts. ‡: the state-of-the-art model.

to 224×224 unless the ResNet-50 \times 16 visual backbone, which utilizes an image size of 384×384 . Crop and random horizontal flip are also adopted to augment the original images for robustness considerations. For BALLAD, we train Phase A for 50 epochs and Phase B for 10 epochs by default unless specified. For the hyperparameters, we set the residual factor λ to 0.2 and the temperature τ to 1.0. The feature dimensions of ResNet-50, ResNet-101, ResNet-50 \times 16 and ViT-B/16 are 1024, 512, 768, 512 respectively.

Evaluation Metrics. We evaluate the models for long-tailed recognition on the balanced test splits and report the commonly used top-1 classification accuracy of *all* classes. Following [30], we divide these classes into three subsets – *many-shot*, *medium-shot*, and *few-shot* categories. Specifically, *many-shot*, *medium-shot*, and *few-shot* are decided according to the amount of instances in each category, namely more than 100 images, 20-100 images, and less than 20 images, respectively.

4.2. Performance Comparison

In this section, we compare the performance of BALLAD with long-tailed recognition approaches that report state-of-the-art results on three benchmark datasets, *i.e.*, ImageNet-LT, Places-LT, and CIFAR100-LT.

ImageNet-LT. Table 1 shows the long-tailed recognition results on ImageNet-LT. We present BALLAD variants with ResNet-50, ResNet-101, ResNet-50 \times 16, and ViT-B/16 as the visual backbone. From the table, we observe that with only 50 + 10 epochs (50 epochs for Phase A and 10 epochs

Method	Backbone	#Pretrain	Many	Medium	Few	All
OLTR [41]	ResNet-152	Y	44.7	37.0	25.3	35.9
cRT [30]	ResNet-152	Y	42	37.6	24.9	36.7
τ -normalized [30]	ResNet-152	Y	37.8	40.7	31.8	37.9
LWS [30]	ResNet-152	Y	40.6	39.1	28.6	37.6
Balanced Softmax [52]	ResNet-152	Y	42.0	39.3	30.5	38.6
ResLT [9]	ResNet-152	Y	39.8	43.6	31.4	39.8
PaCo [10]	ResNet-152	Y	37.5	47.2	33.9	41.2
PaCo† [10]	ResNet-152	Y	36.1	47.9	35.3	41.2
BALLAD	ResNet-50	N	46.7	48.0	42.7	46.5 (+5.3)
	ResNet-101	N	48.0	48.6	46.0	47.9 (+6.7)
	ViT-B/16	N	49.3	50.2	48.4	49.5 (+8.3)
	ResNet-50×16	N	49.4	50.5	46.6	49.3 (+8.1)

Table 2. Long-tailed recognition accuracy on Places-LT for different methods. The red colored numbers represent improvement of overall accuracy compared with the state-of-the-art performance (PaCo with 41.2% overall accuracy). #Pretrain: whether pretrain visual backbone on full ImageNet-2012 or not. †: PaCo variant trained with RandAugment [8].

Method	Backbone	Many	Medium	Few	All
OLTR [41]	ResNet-32	61.8	41.4	17.6	41.2
LDAM+DRW [2]	ResNet-32	61.5	41.7	20.2	42.0
τ -normalized [30]	ResNet-32	65.7	43.6	17.3	43.2
cRT [30]	ResNet-32	64.0	44.8	18.1	43.3
RIDE [62]	ResNet-32	69.3	49.3	26.0	49.1
TADE [72]	ResNet-32	65.4	49.3	29.3	49.8
BALLAD	ResNet-50	62.4	52.3	38.2	51.6 (+1.8)
	ResNet-101	69.5	59.3	47.1	59.2 (+9.4)
	ViT-B/16	84.9	79.7	67.3	77.8 (+28.0)
	ResNet-50×16	74.6	62.8	52.0	63.7 (+13.9)

Table 3. Long-tailed recognition performance comparison on CIFAR100-LT with an imbalance ratio of 100. The red numbers represent the improvement of overall accuracy compared with the state-of-the-art performance (TADE with 49.8% overall accuracy).

for Phase B), our smallest BALLAD variant with ResNet-50 visual backbone can surpass the largest model of the state-of-the-art PaCo [10] using ResNeXt-101 by +7.2%. When gradually increasing the size of visual backbone, we find the performance of BALLAD also enjoys an improvement. It is worth noting that BALLAD with ResNet-50×16 achieves an accuracy of 76.5%, which outperforms other state-of-the-art models with a large margin.

Places-LT. We further evaluate BALLAD on Places-LT dataset and report the results in Table 2. It is a commonly used scheme of previous approaches to pretrain their models on ImageNet-2012 full dataset first to enrich the visual representation before finetuning on Places-LT. However, BALLAD can directly perform training on Places-LT thanks to the additional language representation of contrastive vision-language models. As shown in Table 2, BALLAD with ResNet-50 visual backbone achieves 46.5% accuracy for *all* categories, which beats the state-of-the-art model PaCo with ResNet-152 by +5.3%. This shows BALLAD can not only achieve better performance with smaller visual backbone but also save a great amount of training time by skipping the ImageNet pretraining.

CIFAR100-LT. We also evaluate the models on CIFAR100-LT and show their performances in Table 3. As reported in

Vision	Language	Many	Medium	Few	All
random	random	0.3	0.0	0.0	0.1
random	CLIP	0.3	0.0	0.0	0.1
CLIP	random	36.8	2.9	0.0	15.6
CLIP	CLIP	75.5	56.3	41.0	61.6

Table 4. Ablations of pretrained vision-language weights on ImageNet-LT dataset. *CLIP* means using pre-trained weights as initialization and *random* represents random initialization.

Vision	Language	Many	Medium	Few	All
×	×	59.4	57.5	57.6	58.2
✓	×	70.4	65.4	58.0	66.3
×	✓	70.6	65.4	55.9	66.1
✓	✓	71.3	65.4	54.1	66.1

Table 5. Different methods of finetuning CLIP on ImageNet-LT. "✓" means finetuning and "×" means freezing the parameters of model. *Vision* and *Language* denotes the visual and text encoders of CLIP respectively. All models are finetuned for 50 epochs.

the table, BALLAD outperforms the state-of-the-art expert-based ensemble methods RIDE [63] and TADE [72] by +28.7% and +28.0%, respectively.

4.3. Ablation Studies

In this section, we conduct extensive ablation studies to validate the design choices of BALLAD from three aspects. We first explore how to best utilize vision-language backbone for finetuning. Moreover, we shows the effectiveness of linear adapter and how to make use of linear adapter for better performance. Finally, we demonstrate where and how to conduct data balancing.

4.3.1 Vision-Language Models

We conduct ablations to demonstrate the effectiveness of vision-language backbones as introduced in Section 3.

The Effectiveness of Pretrained Weights. In Table 4, we validate the effectiveness of pretrained CLIP weights compared with random initialized visual and language weights. All the four ablations are conducted on Phase A without data balancing for 50 epochs. The large gaps between random and pretrained CLIP initialization demonstrate the advantage of utilizing pretrained contrastive vision-language models. Besides, we find that visual encoder has much more influence than text encoder on the performance as random initialized vision encoder drops the accuracy close to zero. Note that poor performance of random initialization is primarily attributed to short training periods and pretrained vision-language weights fastening the convergence largely.

Finetune the Vision-Language Model. To empirically discover how to utilize contrastive vision-language models, we probe the finetuning process by freezing the pre-trained image encoder and text encoder respectively. When both

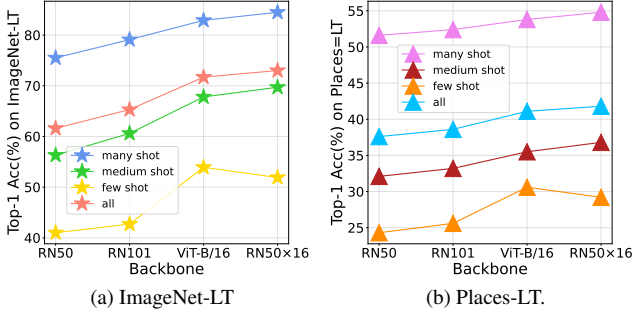


Figure 3. Comparisons between several visual backbones for ImageNet-LT (left) and Places-LT (right).

encoders are frozen, the model directly perform zero-shot predictions. From Table 5, we can easily find the following pattern – as more components are finetuned in CLIP, more accuracy improvement is obtained for *many-shot* categories whereas more accuracy drop happens in *few-shot* division. We hypothesize it is because the *many-shot* classes dominate the visual feature space during finetuning. Therefore, for Phase A, it is necessary to adapt CLIP on specific long-tailed dataset as much as possible, and we choose to finetune both the vision and language branches of CLIP.

Visual Backbones. We try CLIP with different visual backbones to explore its influence on final performance of BALLAD. We report the Phase A results of different backbones in Figure 3 on both ImageNet-LT and Places-LT benchmarks. When the visual backbone becomes deeper and larger, the finetuned performance is also gradually improved for *all*, *many-shot*, and *medium-shot* categories. Surprisingly, the Vision Transformer structure [14] achieves the best accuracy in *few-shot* subset, probably owing to multi-head self-attention mechanism’s ability in capturing minor features.

4.3.2 Linear Adapter

We validate the effectiveness of adopting linear adapter in Phase B and explore the key factors that determines the performance of linear adapter.

The Effectiveness of Linear Adapter. We design ablations to demonstrate the influence of linear adapter. First, we freeze the parameters of CLIP and finetune the linear adapter for 10 epochs to mix the original zero-shot visual embedding with the corresponding finetuned visual features via residual connection. As illustrated in Figure 4, the simple 10-epoch training improves the performance from 58.2% to 61.8% even without data balancing. Moreover, we finetune both the visual and language encoders of CLIP for 50 epochs and then finetune the linear adapter for another 10 epochs with CLIP parameters fixed. Compared with an equal 60-epoch training scheme of finetuning the visual and language encoder of the CLIP, an extra 10-epoch finetuning of linear adapter based on 50-epoch finetuning of CLIP backbone can further boost the top-1 accuracy from 66.4% to 67.2%.

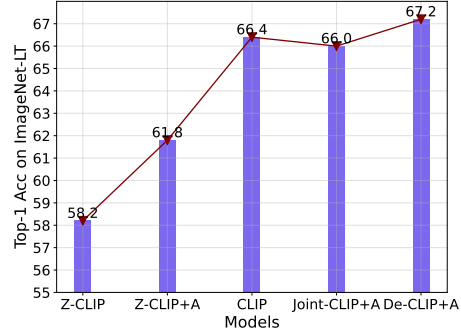


Figure 4. Ablations of effectiveness of Linear Adapter and decouple finetuning. *Z-CLIP*: zero-shot CLIP model; *Z-CLIP+A*: finetune adapter based on zero-shot CLIP; *CLIP*: directly finetune CLIP; *Joint-CLIP+A*: jointly finetune CLIP and adapter; *De-CLIP+A*: the BALLAD style which decouples the CLIP and adapter finetuning into two phases.

V-Adapter	L-Adapter	Many	Medium	Few	All
✓	×	71.0	66.3	59.5	67.2
×	✓	71.0	66.2	59.0	67.0
✓	✓	70.6	66.2	58.4	66.8

Table 6. Variants of linear adapter. *V-Adapter* and *L-Adapter* represents using linear adapter layer to adapt visual and language encoders respectively. All results are trained on ImageNet-LT for 10 epochs.

Should the Finetuning of CLIP and Linear Adapter be Decoupled? As mentioned in Section 3 and illustrated in Figure 2, we decouple the training process into two phases – in Phase A, we train both the vision and language encoder of CLIP based on pre-trained weights; in Phase B, we freeze the parameters of visual and language encoders while only finetuning the linear adapter. An alternative scheme is to jointly train the CLIP and linear adapter rather than decoupling the training processes. According to Figure 4, joint training of CLIP and linear adapter (*Joint-CLIP+A*) leads to a 0.4% accuracy drop compared with directly finetuning CLIP without adapter (*CLIP*). In contrast, the decoupled training of CLIP and linear adapter (*De-CLIP+A*) can largely boost the accuracy from 66.0% to 67.2% and the ascent mainly comes from tail classes, which is up to 6.0%. We visualize the joint and decoupling training schemes using t-SNE [60] and present the results in the supplementary. Compared with joint training, decoupled training better separates the tail-class feature embeddings from head-classes. This demonstrates that the proposed decoupled training of vision-language model and adapter is effective to handle long-tailed distribution.

Variants of Linear Adapter. Since CLIP has dual encoders, the auxiliary linear adapter could be added to either or both of the two branches. As reported in Table 6, we try linear adapter for adapting visual and language encoders

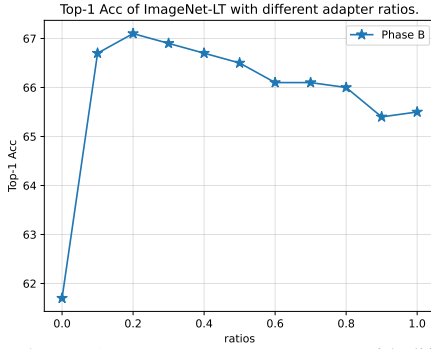


Figure 5. The top-1 accuracy on ImageNet-LT with different values of residual factor λ in Phase B of BALLAD.

respectively. From the table, we can find that applying the linear adapter to the visual branch of CLIP achieves the best overall performance and is the optimal choice.

Hyperparameters of the Linear Adapter. Moreover, we explore the influence of linear adapter’s residual factor λ . λ determines the importance of new knowledge obtained from finetuning the linear adapter. Note that when λ equals to 1.0, the classification is fully determined by the adapted image features. We explore different values of λ from 0.0 to 1.0 and conduct the ablations of Phase B finetuning on ImageNet-LT. As shown in Figure 5, the best performance of linear adapter can be obtained when λ is around 0.2, with a top-1 accuracy of 67.1% on ImageNet-LT. The empirical results reveal the knowledge of finetuned CLIP is already good enough to handle most cases, a slight and balanced adaptation would further improve the performance.

4.3.3 Balancing Methods

Balancing methods can alleviate the severe performance degradation due to class imbalance. In this section, we explore different balancing methods for BALLAD to reveal two significant problems: 1) where to utilize balancing methods, and 2) which balancing methods to apply.

Where to balance. Here, we compare balancing the long-tailed data distribution on either or both of two phases. The experiments are performed on ImageNet-LT and Places-LT datasets with ResNet-50-backed CLIP. As mentioned earlier, *many-shot* categories dominate the feature space of long-tailed distribution. The performance drops of *many-shot* categories on both datasets, as reported in Table 7, suggest that balancing during Phase A tends to sacrifice *many-shot* representations. Since Phase A is mainly designed for updating representations on a new domain, we thereby abandon Phase-A data balancing. When applying balancing strategies to Phase B alone, BALLAD can achieve a more balanced performance for different shots and improve the overall top-1 accuracy thanks to the rich features learned from Phase A.

How to balance. Furthermore, we explore different sampling strategies including class-balanced sampling, square-

Dataset	Balance		Many	Medium	Few	All
	Phase A	Phase B				
ImageNet-LT	×	×	77.3	57.4	39.0	62.6
	✓	×	76.6	58.4	42.7	63.3
	✓	✓	70.7	66.2	58.5	66.9
	×	✓	71.0	66.3	59.5	67.2
Places-LT	×	×	52.7	32.9	23.4	38.2
	✓	×	51.3	33.2	25.5	38.2
	✓	✓	44.6	46.7	44.1	45.5
	×	✓	46.7	48.0	42.7	46.5

Table 7. Where to employ balance strategies ablations. On both ImageNet-LT and Places-LT, balance only in Phase B make BALLAD perform the best.

Balance Methods	Many	Medium	Few	All
Class-balanced	71.0	66.3	59.5	67.2
Square-root	75.2	62.8	50.9	66.0
Mix-balanced	72.6	64.9	59.1	67.1

Table 8. Comparison of different balanced sampling strategies on ImageNet-LT.

root sampling and mix-balanced sampling for Phase B. Class-balanced sampling samples the categories from original dataset in equal probability rather than the natural instance-balanced sampling which selects instances regardless of classes. The process can be decoupled into two steps – first selecting classes equally from the list of categories and then randomly sampling a data point from the selected class. Square-root sampling [43] first computes the square-root of the number of head classes, then re-normalize and conduct sampling according to the resulting distribution. Mix-balanced sampling combines the instance-balanced sampling and class-balanced sampling, thus takes advantage of both strategies to avoid overfitting at early epochs and underfitting at late epochs. Motivated by the [30], we adopt a soft version of mix-balanced sampling to dynamically interpolates between instance-balanced sampling and class-balanced sampling as learning progresses. As shown in Table 8, class-balanced sampling can best benefit *medium-shot* and *few-shot* categories. Thus we adopt class-balanced sampling as the balancing method of BALLAD.

5. Conclusion

In this paper, we proposed BALLAD which tackles long-tailed recognition by leveraging contrastive vision-language models. We decouple BALLAD into two phases for training with long-tailed and balanced samples respectively. We first continue pretraining with contrastive loss to fully utilize abundant data to update visual-language representation on specific domains. After that, we employ an auxiliary linear adapter to refine the visual representation of tail classes. We hope our simple BALLAD baseline could stimulate more future researches on exploring vision-language models for

long-tailed recognition.

References

- [1] Stanislaw Antol, Aishwarya Agrawal, Jiasen Lu, Margaret Mitchell, Dhruv Batra, C Lawrence Zitnick, and Devi Parikh. Vqa: Visual question answering. In *Proceedings of the IEEE international conference on computer vision*, pages 2425–2433, 2015. 2
- [2] Kaidi Cao, Colin Wei, Adrien Gaidon, Nikos Arechiga, and Tengyu Ma. Learning imbalanced datasets with label-distribution-aware margin loss. In *Advances in Neural Information Processing Systems*, pages 1567–1578, 2019. 5, 6
- [3] Mathilde Caron, Ishan Misra, Julien Mairal, Priya Goyal, Piotr Bojanowski, and Armand Joulin. Unsupervised learning of visual features by contrasting cluster assignments. In *Advances in Neural Information Processing Systems*, 2020. 2
- [4] Mathilde Caron, Hugo Touvron, Ishan Misra, Hervé Jégou, Julien Mairal, Piotr Bojanowski, and Armand Joulin. Emerging properties in self-supervised vision transformers. In *Proceedings of the International Conference on Computer Vision (ICCV)*, 2021. 2
- [5] Liang-Chieh Chen, George Papandreou, Iasonas Kokkinos, Kevin Murphy, and Alan L Yuille. Deeplab: Semantic image segmentation with deep convolutional nets, atrous convolution, and fully connected crfs. *IEEE transactions on pattern analysis and machine intelligence*, 40(4):834–848, 2017. 1
- [6] Ting Chen, Simon Kornblith, Mohammad Norouzi, and Geoffrey Hinton. A simple framework for contrastive learning of visual representations. In *International conference on machine learning*, pages 1597–1607. PMLR, 2020. 2
- [7] Yen-Chun Chen, Linjie Li, Licheng Yu, Ahmed El Kholy, Faisal Ahmed, Zhe Gan, Yu Cheng, and Jingjing Liu. Uniter: Learning universal image-text representations. 2019. 2
- [8] Ekin Dogus Cubuk, Barret Zoph, Jon Shlens, and Quoc Le. Randaugment: Practical automated data augmentation with a reduced search space. In *Advances in Neural Information Processing Systems*, 2020. 6
- [9] Jiequan Cui, Shu Liu, Zhuotao Tian, Zhisheng Zhong, and Jiaya Jia. Reslt: Residual learning for long-tailed recognition. *arXiv preprint arXiv:2101.10633*, 2021. 2, 3, 5, 6
- [10] Jiequan Cui, Zhisheng Zhong, Shu Liu, Bei Yu, and Jiaya Jia. Parametric contrastive learning. In *Proceedings of the IEEE/CVF International Conference on Computer Vision*, pages 715–724, 2021. 1, 2, 3, 4, 5, 6
- [11] Yin Cui, Menglin Jia, Tsung-Yi Lin, Yang Song, and Serge Belongie. Class-balanced loss based on effective number of samples. In *Proceedings of the IEEE/CVF conference on computer vision and pattern recognition*, pages 9268–9277, 2019. 5
- [12] Jia Deng, Wei Dong, Richard Socher, Li-Jia Li, Kai Li, and Li Fei-Fei. Imagenet: A large-scale hierarchical image database. In *2009 IEEE conference on computer vision and pattern recognition*, pages 248–255. Ieee, 2009. 1, 5
- [13] Qi Dong, Shaogang Gong, and Xiatian Zhu. Class rectification hard mining for imbalanced deep learning. In *Proceedings of the IEEE International Conference on Computer Vision*, pages 1851–1860, 2017. 3
- [14] Alexey Dosovitskiy, Lucas Beyer, Alexander Kolesnikov, Dirk Weissenborn, Xiaohua Zhai, Thomas Unterthiner, Mostafa Dehghani, Matthias Minderer, Georg Heigold, Sylvain Gelly, Jakob Uszkoreit, and Neil Houlsby. An image is worth 16x16 words: Transformers for image recognition at scale. In *International Conference on Learning Representations*, 2021. 7
- [15] Peng Gao, Shijie Geng, Renrui Zhang, Teli Ma, Rongyao Fang, Yongfeng Zhang, Hongsheng Li, and Yu Qiao. Clip-adapter: Better vision-language models with feature adapters. *arXiv preprint arXiv:2110.04544*, 2021. 3
- [16] Peng Gao, Zhengkai Jiang, Haoxuan You, Pan Lu, Steven CH Hoi, Xiaogang Wang, and Hongsheng Li. Dynamic fusion with intra-and inter-modality attention flow for visual question answering. In *Proceedings of the IEEE/CVF Conference on Computer Vision and Pattern Recognition*, pages 6639–6648, 2019. 2
- [17] Tianyu Gao, Xingcheng Yao, and Danqi Chen. Simcse: Simple contrastive learning of sentence embeddings. In *Proceedings of the 2020 Conference on Empirical Methods in Natural Language Processing (EMNLP)*, 2021. 2
- [18] Suchin Gururangan, Ana Marasović, Swabha Swayamdipta, Kyle Lo, Iz Beltagy, Doug Downey, and Noah A Smith. Don’t stop pretraining: adapt language models to domains and tasks. *arXiv preprint arXiv:2004.10964*, 2020. 4
- [19] Kaiming He, Haoqi Fan, Yuxin Wu, Saining Xie, and Ross Girshick. Momentum contrast for unsupervised visual representation learning. In *Proceedings of the IEEE/CVF Conference on Computer Vision and Pattern Recognition*, pages 9729–9738, 2020. 2
- [20] Kaiming He, Georgia Gkioxari, Piotr Dollár, and Ross Girshick. Mask r-cnn. In *Proceedings of the IEEE international conference on computer vision*, pages 2961–2969, 2017. 1
- [21] Kaiming He, Xiangyu Zhang, Shaoqing Ren, and Jian Sun. Deep residual learning for image recognition. In *Proceedings of the IEEE conference on computer vision and pattern recognition*, pages 770–778, 2016. 1
- [22] Youngkyu Hong, Seungju Han, Kwanghee Choi, Seokjun Seo, Beomsu Kim, and Buru Chang. Disentangling label distribution for long-tailed visual recognition. In *Proceedings of the IEEE/CVF Conference on Computer Vision and Pattern Recognition*, pages 6626–6636, 2021. 2, 3
- [23] Neil Houlsby, Andrei Giurgiu, Stanislaw Jastrzebski, Bruna Morrone, Quentin De Laroussilhe, Andrea Gesmundo, Mona Attariyan, and Sylvain Gelly. Parameter-efficient transfer learning for nlp. In *International Conference on Machine Learning*, pages 2790–2799. PMLR, 2019. 4
- [24] Ronghang Hu, Piotr Dollár, Kaiming He, Trevor Darrell, and Ross Girshick. Learning to segment every thing. In *Proceedings of the IEEE Conference on Computer Vision and Pattern Recognition*, pages 4233–4241, 2018. 1
- [25] Chen Huang, Yining Li, Chen Change Loy, and Xiaoou Tang. Learning deep representation for imbalanced classification. In *Proceedings of the IEEE conference on computer vision and pattern recognition*, pages 5375–5384, 2016. 3

- [26] Chao Jia, Yinfei Yang, Ye Xia, Yi-Ting Chen, Zarana Parekh, Hieu Pham, Quoc V Le, Yunhsuan Sung, Zhen Li, and Tom Duerig. Scaling up visual and vision-language representation learning with noisy text supervision. In *International Conference on Machine Learning*, 2021. 2, 4
- [27] Zhengbao Jiang, Frank F Xu, Jun Araki, and Graham Neubig. How can we know what language models know? *Transactions of the Association for Computational Linguistics*, 8:423–438, 2020. 12
- [28] Bingyi Kang, Yu Li, Sa Xie, Zehuan Yuan, and Jiashi Feng. Exploring balanced feature spaces for representation learning. In *International Conference on Learning Representations*, 2021. 3
- [29] Bingyi Kang, Zhuang Liu, Xin Wang, Fisher Yu, Jiashi Feng, and Trevor Darrell. Few-shot object detection via feature reweighting. In *Proceedings of the IEEE/CVF International Conference on Computer Vision*, pages 8420–8429, 2019. 2, 3
- [30] Bingyi Kang, Saining Xie, Marcus Rohrbach, Zhicheng Yan, Albert Gordo, Jiashi Feng, and Yannis Kalantidis. Decoupling representation and classifier for long-tailed recognition. In *International Conference on Learning Representations*, 2020. 2, 3, 4, 5, 6, 8
- [31] Will Kay, Joao Carreira, Karen Simonyan, Brian Zhang, Chloe Hillier, Sudheendra Vijayanarasimhan, Fabio Viola, Tim Green, Trevor Back, Paul Natsev, et al. The kinetics human action video dataset. *arXiv preprint arXiv:1705.06950*, 2017. 1
- [32] Jin-Hwa Kim, Jaehyun Jun, and Byoung-Tak Zhang. Bilinear attention networks. *arXiv preprint arXiv:1805.07932*, 2018. 2
- [33] Ranjay Krishna, Yuke Zhu, Oliver Groth, Justin Johnson, Kenji Hata, Joshua Kravitz, Stephanie Chen, Yannis Kalantidis, Li-Jia Li, David A Shamma, et al. Visual genome: Connecting language and vision using crowdsourced dense image annotations. *International journal of computer vision*, 123(1):32–73, 2017. 1
- [34] Xiang Lisa Li and Percy Liang. Prefix-tuning: Optimizing continuous prompts for generation. *arXiv preprint arXiv:2101.00190*, 2021. 12
- [35] Yangguang Li, Feng Liang, Lichen Zhao, Yufeng Cui, Wanli Ouyang, Jing Shao, Fengwei Yu, and Junjie Yan. Supervision exists everywhere: A data efficient contrastive language-image pre-training paradigm. *arXiv preprint arXiv:2110.05208*, 2021. 2
- [36] Tsung-Yi Lin, Piotr Dollár, Ross Girshick, Kaiming He, Bharath Hariharan, and Serge Belongie. Feature pyramid networks for object detection. In *Proceedings of the IEEE conference on computer vision and pattern recognition*, pages 2117–2125, 2017. 1
- [37] Tsung-Yi Lin, Priya Goyal, Ross Girshick, Kaiming He, and Piotr Dollár. Focal loss for dense object detection. In *Proceedings of the IEEE international conference on computer vision*, pages 2980–2988, 2017. 3
- [38] Tsung-Yi Lin, Michael Maire, Serge Belongie, James Hays, Pietro Perona, Deva Ramanan, Piotr Dollár, and C Lawrence Zitnick. Microsoft coco: Common objects in context. In *European conference on computer vision*, pages 740–755. Springer, 2014. 1
- [39] Jialun Liu, Yifan Sun, Chuchu Han, Zhaopeng Dou, and Wenhui Li. Deep representation learning on long-tailed data: A learnable embedding augmentation perspective. In *Proceedings of the IEEE/CVF Conference on Computer Vision and Pattern Recognition*, pages 2970–2979, 2020. 3
- [40] Shu Liu, Lu Qi, Haifang Qin, Jianping Shi, and Jiaya Jia. Path aggregation network for instance segmentation. In *Proceedings of the IEEE conference on computer vision and pattern recognition*, pages 8759–8768, 2018. 1
- [41] Ziwei Liu, Zhongqi Miao, Xiaohang Zhan, Jiayun Wang, Boqing Gong, and Stella X Yu. Large-scale long-tailed recognition in an open world. In *Proceedings of the IEEE/CVF Conference on Computer Vision and Pattern Recognition*, pages 2537–2546, 2019. 2, 3, 5, 6, 12
- [42] Jonathan Long, Evan Shelhamer, and Trevor Darrell. Fully convolutional networks for semantic segmentation. In *Proceedings of the IEEE conference on computer vision and pattern recognition*, pages 3431–3440, 2015. 1
- [43] Dhruv Mahajan, Ross Girshick, Vignesh Ramanathan, Kaiming He, Manohar Paluri, Yixuan Li, Ashwin Bharambe, and Laurens Van Der Maaten. Exploring the limits of weakly supervised pretraining. In *Proceedings of the European conference on computer vision (ECCV)*, pages 181–196, 2018. 8
- [44] Aditya Krishna Menon, Sadeep Jayasumana, Ankit Singh Rawat, Himanshu Jain, Andreas Veit, and Sanjiv Kumar. Long-tail learning via logit adjustment. In *International Conference on Learning Representations*, 2021. 2, 3
- [45] Medhini Narasimhan, Anna Rohrbach, and Trevor Darrell. Clip-it! language-guided video summarization. In *Advances in Neural Information Processing Systems*, 2021. 3
- [46] Duy-Kien Nguyen and Takayuki Okatani. Improved fusion of visual and language representations by dense symmetric co-attention for visual question answering. In *Proceedings of the IEEE Conference on Computer Vision and Pattern Recognition*, pages 6087–6096, 2018. 2
- [47] Aaron van den Oord, Yazhe Li, and Oriol Vinyals. Representation learning with contrastive predictive coding. *arXiv preprint arXiv:1807.03748*, 2018. 2
- [48] Wanli Ouyang, Xiaogang Wang, Cong Zhang, and Xiaokang Yang. Factors in finetuning deep model for object detection with long-tail distribution. In *Proceedings of the IEEE conference on computer vision and pattern recognition*, pages 864–873, 2016. 3
- [49] Vilfredo Pareto. *Cours d'économie politique*. Librairie Droz, 1964. 1
- [50] Fabio Petroni, Tim Rocktäschel, Sebastian Riedel, Patrick Lewis, Anton Bakhtin, Yuxiang Wu, and Alexander Miller. Language models as knowledge bases? In *Proceedings of the 2019 Conference on Empirical Methods in Natural Language Processing and the 9th International Joint Conference on Natural Language Processing (EMNLP-IJCNLP)*, pages 2463–2473, 2019. 12
- [51] Alec Radford, Jong Wook Kim, Chris Hallacy, Aditya Ramesh, Gabriel Goh, Sandhini Agarwal, Girish Sastry,

- Amanda Aspell, Pamela Mishkin, Jack Clark, et al. Learning transferable visual models from natural language supervision. In *International Conference on Machine Learning*, 2021. 2, 4, 5, 12
- [52] Jiawei Ren, Cunjun Yu, Shunan Sheng, Xiao Ma, Haiyu Zhao, Shuai Yi, and Hongsheng Li. Balanced meta-softmax for long-tailed visual recognition. *arXiv preprint arXiv:2007.10740*, 2020. 5, 6
- [53] Shaoqing Ren, Kaiming He, Ross Girshick, and Jian Sun. Faster r-cnn: Towards real-time object detection with region proposal networks. *Advances in neural information processing systems*, 28:91–99, 2015. 1
- [54] Dvir Samuel and Gal Chechik. Distributional robustness loss for long-tail learning. In *Proceedings of the IEEE/CVF International Conference on Computer Vision*, pages 9495–9504, 2021. 2, 3
- [55] Lei Shi, Kai Shuang, Shijie Geng, Peng Su, Zhengkai Jiang, Peng Gao, Zuohui Fu, Gerard de Melo, and Sen Su. Contrastive visual-linguistic pretraining. *arXiv preprint arXiv:2007.13135*, 2020. 2
- [56] Taylor Shin, Yasaman Razeghi, Robert L Logan IV, Eric Wallace, and Sameer Singh. Eliciting knowledge from language models using automatically generated prompts. In *Proceedings of the 2020 Conference on Empirical Methods in Natural Language Processing (EMNLP)*, pages 4222–4235, 2020. 12
- [57] Mohit Shridhar, Lucas Manuelli, and Dieter Fox. Cliport: What and where pathways for robotic manipulation. In *Proceedings of the 5th Conference on Robot Learning (CoRL)*, 2021. 3
- [58] Karen Simonyan and Andrew Zisserman. Very deep convolutional networks for large-scale image recognition. In *International Conference on Learning Representations*, 2015. 1
- [59] Kaihua Tang, Jianqiang Huang, and Hanwang Zhang. Long-tailed classification by keeping the good and removing the bad momentum causal effect. In *Advances in Neural Information Processing Systems*, 2020. 2, 3
- [60] Laurens Van der Maaten and Geoffrey Hinton. Visualizing data using t-sne. *Journal of machine learning research*, 9(11), 2008. 7, 13
- [61] Mengmeng Wang, Jiazheng Xing, and Yong Liu. Actionclip: A new paradigm for video action recognition. *arXiv preprint arXiv:2109.08472*, 2021. 3
- [62] Xudong Wang, Long Lian, Zhongqi Miao, Ziwei Liu, and Stella Yu. Long-tailed recognition by routing diverse distribution-aware experts. In *International Conference on Learning Representations*, 2020. 5, 6
- [63] Xudong Wang, Long Lian, Zhongqi Miao, Ziwei Liu, and Stella Yu. Long-tailed recognition by routing diverse distribution-aware experts. In *International Conference on Learning Representations*, 2021. 3, 5, 6
- [64] Tz-Ying Wu, Pedro Morgado, Pei Wang, Chih-Hui Ho, and Nuno Vasconcelos. Solving long-tailed recognition with deep realistic taxonomic classifier. In *European Conference on Computer Vision*, pages 171–189. Springer, 2020. 3
- [65] Saining Xie, Ross Girshick, Piotr Dollár, Zhuowen Tu, and Kaiming He. Aggregated residual transformations for deep neural networks. In *Proceedings of the IEEE conference on computer vision and pattern recognition*, pages 1492–1500, 2017. 1
- [66] Hu Xu, Gargi Ghosh, Po-Yao Huang, Dmytro Okhonko, Armen Aghajanyan, Florian Metze, Luke Zettlemoyer, and Christoph Feichtenhofer. Videoclip: Contrastive pre-training for zero-shot video-text understanding. In *Proceedings of the 2020 Conference on Empirical Methods in Natural Language Processing (EMNLP)*, 2021. 3
- [67] Xi Yin, Xiang Yu, Kihyuk Sohn, Xiaoming Liu, and Manmohan Chandraker. Feature transfer learning for face recognition with under-represented data. In *Proceedings of the IEEE/CVF Conference on Computer Vision and Pattern Recognition*, pages 5704–5713, 2019. 3
- [68] Zhou Yu, Jun Yu, Yuhao Cui, Dacheng Tao, and Qi Tian. Deep modular co-attention networks for visual question answering. In *Proceedings of the IEEE/CVF Conference on Computer Vision and Pattern Recognition*, pages 6281–6290, 2019. 2
- [69] Andy Zeng, Pete Florence, Jonathan Tompson, Stefan Welker, Jonathan Chien, Maria Attarian, Travis Armstrong, Ivan Krasin, Dan Duong, Vikas Sindhwani, and Johnny Lee. Transporter networks: Rearranging the visual world for robotic manipulation. In *Proceedings of the 4th Conference on Robot Learning (CoRL)*, 2020. 3
- [70] Songyang Zhang, Zeming Li, Shipeng Yan, Xuming He, and Jian Sun. Distribution alignment: A unified framework for long-tail visual recognition. In *Proceedings of the IEEE/CVF Conference on Computer Vision and Pattern Recognition*, pages 2361–2370, 2021. 2, 3
- [71] Xiao Zhang, Zhiyuan Fang, Yandong Wen, Zhifeng Li, and Yu Qiao. Range loss for deep face recognition with long-tailed training data. In *Proceedings of the IEEE International Conference on Computer Vision*, pages 5409–5418, 2017. 3
- [72] Yifan Zhang, Bryan Hooi, Lanqing Hong, and Jiashi Feng. Test-agnostic long-tailed recognition by test-time aggregating diverse experts with self-supervision. *arXiv preprint arXiv:2107.09249*, 2021. 2, 3, 6
- [73] Yifan Zhang, Bingyi Kang, Bryan Hooi, Shuicheng Yan, and Jiashi Feng. Deep long-tailed learning: A survey. *arXiv preprint arXiv:2110.04596*, 2021. 2, 3
- [74] Hengshuang Zhao, Jianping Shi, Xiaojuan Qi, Xiaogang Wang, and Jiaya Jia. Pyramid scene parsing network. In *Proceedings of the IEEE conference on computer vision and pattern recognition*, pages 2881–2890, 2017. 1
- [75] Boyan Zhou, Quan Cui, Xiu-Shen Wei, and Zhao-Min Chen. Bbn: Bilateral-branch network with cumulative learning for long-tailed visual recognition. In *Proceedings of the IEEE/CVF Conference on Computer Vision and Pattern Recognition*, pages 9719–9728, 2020. 2, 3
- [76] Bolei Zhou, Agata Lapedriza, Aditya Khosla, Aude Oliva, and Antonio Torralba. Places: A 10 million image database for scene recognition. *IEEE transactions on pattern analysis and machine intelligence*, 40(6):1452–1464, 2017. 5
- [77] Linchao Zhu and Yi Yang. Inflated episodic memory with region self-attention for long-tailed visual recognition. In *Proceedings of the IEEE/CVF Conference on Computer Vision and Pattern Recognition*, pages 4344–4353, 2020. 3

[78] George Kingsley Zipf. *Human behavior and the principle of least effort: An introduction to human ecology*. Addison-Wesley Press, Inc., 1949. 1

Appendices

This supplementary file includes more details and results of BALLAD that were not contained in the main manuscript due to the limited paper size. We start with elaborating the two-phase training of BALLAD in Appendix A. Then we provide the zero-shot long-tailed recognition performance of the vision-language model CLIP in three benchmark datasets (Appendix B). Moreover, we perform ablations of different text prompts in Appendix C. Appendix D shows visualization results of the decoupled training of CLIP and linear adapter as discussed in Sec. 4.3.2 in main manuscript.

A. Algorithm

We provide the pseudo code of training BALLAD as shown in Algorithm 1. In phase A, we keep training the vision-language model, updating parameters of both visual and language encoders. Afterward, in phase B, we train a single linear adapter with vision-language model frozen to adapt visual features in a balanced way.

B. Zero-shot Performance

The zero-shot long-tailed recognition performances on three benchmark datasets are presented in Table 9. The red numbers show how much BALLAD has improved compared with zero-shot CLIP results. It illustrates the training scheme of BALLAD is effective as raising the initial vision-language model by a large margin (+12.2% maximally).

C. Text Prompting

Prompt engineering is initially proposed for knowledge probing in large pretrained language models [27, 34, 50, 56]. Prompting is adding extra instructions to task inputs to generate specific outputs from pretrained language model. In this paper, we utilize manually designed prompts following CLIP [51]. Specifically, a prompt template like *a photo of a {CLASS}* is adopted to all experiments reported in main manuscript. However, CLIP [51] claims that ensembling several classifiers using different hand-crafted prompts as follows can improve the performance of zero-shot tasks.

- itap of a {CLASS}.
- a bad photo of the {CLASS}.
- a origami {CLASS}.
- a photo of the large {CLASS}.
- a {CLASS} in the video game.

Algorithm 1 Two-phases training of BALLAD

Require: Training samples $\{(I, y)\}$, visual and language encoder $\mathcal{V}_{\text{enc}}, \mathcal{L}_{\text{enc}}$, linear adapter $\mathcal{L}\mathcal{A}$
Initialize $\mathcal{V}_{\text{enc}}, \mathcal{L}_{\text{enc}}$ with web-data pretrained parameters Θ_v and Θ_l
for epoch = 1, ..., N_A **do** ▷ Phase A
 for minibatch $B \in \{(I, y)\}$ **do**
 $f_v \leftarrow \mathcal{V}_{\text{enc}}(I) \in \mathbb{R}^{d_v}$
 $T \leftarrow \text{tokenize}(y)$
 $f_l \leftarrow \mathcal{L}_{\text{enc}}(T) \in \mathbb{R}^{d_l}$
 Project into embedding space \mathbf{u}, \mathbf{v} as Eq.(1)
 $p_i \leftarrow \frac{\exp(\mathbf{v}^\top \mathbf{u}_i)/\tau}{\sum_{j=1}^K \exp(\mathbf{v}^\top \mathbf{u}_j)/\tau}$
 Update Θ_v and Θ_l
 end for
end for
Initialize Θ_{LA} randomly for $\mathcal{L}\mathcal{A}$ ▷ Phase B
Freeze Θ_v and Θ_l
for epoch = 1, ..., N_B **do**
 for minibatch $B \in \{\text{Balanced}(I, y)\}$ **do**
 $f_v \leftarrow \lambda \mathcal{L}\mathcal{A}(\mathcal{V}_{\text{enc}}(I)) + (1 - \lambda) \mathcal{V}_{\text{enc}}(I) \in \mathbb{R}^{d_v}$
 $T \leftarrow \text{tokenize}(y)$
 $f_l \leftarrow \mathcal{L}_{\text{enc}}(T) \in \mathbb{R}^{d_l}$
 Project into embedding space \mathbf{u}, \mathbf{v} as Eq.(1)
 $p_i \leftarrow \frac{\exp(\mathbf{v}^\top \mathbf{u}_i)/\tau}{\sum_{j=1}^K \exp(\mathbf{v}^\top \mathbf{u}_j)/\tau}$
 Update Θ_{LA}
 end for
end for

- art of the {CLASS}.
- a photo of the small {CLASS}.

Therefore, we perform ablations on ensembling the multiple prompts and randomly choosing one of them for language model training. Ablations are conducted on ImageNet-LT benchmark [41] with ResNet-50 visual backbone. Results are reported in Table 10. Surprisingly, prompts ensembling decays performance from 67.2% to 66.8% rather than raising accuracy. Randomly choosing a template from above seven prompts also results in performance drop, by 0.3% overall accuracy. We hypothesize different prompting templates from multiple views may confuse the pretrained language model finetuning, which is different from zero-shot task. Thus, we choose a single template *a photo of a {CLASS}* in all our ablations.

D. Visualization

As discussed in Sec. 4.3.2 in main manuscript, decoupled training of vision-language model and linear adapter largely boost the performance, especially for few-shot categories. We visualize the classification space of several

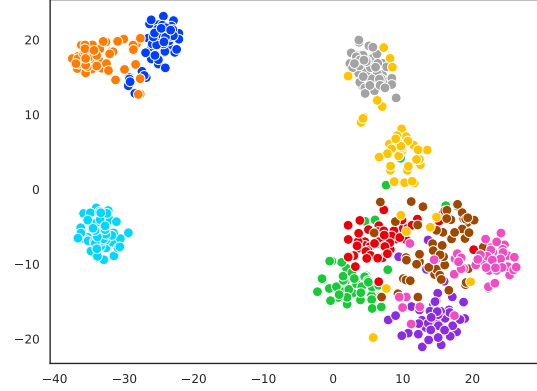
Visual Backbone	ImageNet-LT		Places-LT		CIFAR100-LT	
	zero-shot	BALLAD	zero-shot	BALLAD	zero-shot	BALLAD
ResNet-50	58.2	67.2 (+9)	35.3	46.5 (+11.2)	40.2	51.6 (+11.4)
ResNet-101	61.2	70.5 (+9.3)	36.2	47.9 (+11.7)	47.8	59.2 (+11.4)
ViT-B/16	66.7	75.7 (+9)	37.8	49.5 (+11.7)	66.4	77.8 (+11.4)
ResNet-50×16	69.0	76.5 (+7.5)	37.1	49.3 (+12.2)	52.9	63.7 (+10.8)

Table 9. Top-1 accuracy of zero-shot CLIP and BALLAD-training.

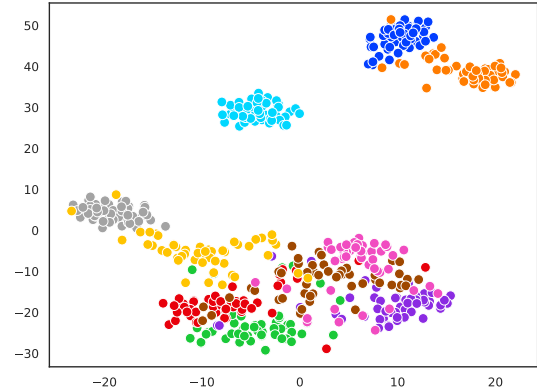
Text Prompts	Many	Medium	Few	All
Single prompt	71.0	66.3	59.5	67.2
Random single prompt	70.5	66.1	59.8	66.9
Ensemble prompts	70.5	66.0	59.5	66.8

Table 10. Comparison of different balanced sampling strategies on ImageNet-LT.

few-shot categories using t-SNE [60] as shown in Fig. 6. It is clearly illustrated in Sub-figure (a) that decoupled training achieves much more obvious separation boundary among different classes, especially for some easily confusing ones such as *kingsnake* (purple), *water snake* (brown) and *sea snake* (pink).



(a) Decoupled training.



(b) Joint training.



(c) Legends

Figure 6. Comparisons of training vision-language model and linear adapter decoupled and jointly.